Prognosis & health management for the prediction of UAV flight endurance

Ricardo Schacht Rodriguez, Jean-Christophe Ponsart, Carlos Daniel Garcia-Beltran, Carlos Manuel Astorga-Zaragoza

Prognosis & Health Management for the prediction of UAV flight endurance ⋆

R. Schacht-Rodríguez [*,**] **J.-C. Ponsart** [**]
C. D. García-Beltrán [*] **C. M. Astorga-Zaragoza** [*]

[*] *Tecnológico Nacional de México, TecNM. Centro Nacional de Investigación y Desarrollo Tecnológico, CENIDET, Internado Palmira s/n Col. Palmira CP 62490, Cuernavaca, Mor. México. (e-mail, rschacht@, cgarcia@, astorga@cenidet.edu.mx).*
[**] *Université de Lorraine, CRAN CNRS, UMR 7039, Campus Sciences, B.P. 70239, 54506 Vandoeuvre-lès-Nancy Cedex France (e-mail: ricardo.schacht-rodriguez@, Jean-Christophe.Ponsart@univ-lorraine.fr)*

Abstract: In this work, a Model-based Prognosis algorithm to predict the *Flight Endurance* (FE) and the *Remaining Mission Time* (RMT) for a class of multirotor UAVs powered by Lithium Polymer (Li-Po) batteries is presented. A *Safety Voltage Threshold* (SVT) in the State of Charge (SoC) of the battery is established before reaching of End of Discharge (EoD), and the SVT is defined taking into account the existing relationship between the voltage and the SoC of the battery. The FE is predicted by forecasting when the SVT is reached and the RMT is computed as the difference between the FE and the actual time. The prediction is developed in three sequential steps: 1) estimation of the battery SoC, 2) propagation and prediction of the estimated SoC in the future to reach the SVT, and 3) updating the prediction. The Model-based Prognosis algorithm is based on the mathematical model of the UAV propulsion system, which is made up by a set of BrushLess DC motors and a Li-Po battery. The effectiveness of the proposed algorithm was tested in simulation and the results obtained demonstrate the efficacy of the proposed method to accurately predict the FE and RMT during the development of a mission.

Keywords: Prediction methods, Extended Kalman Filters, Mobile robots, Threshold voltage, Energy dependence

1. INTRODUCTION

Nowadays, the use of Lithium Polymer (Li-Po) battery as powertrain for multirotor UAVs with capabilities of vertical take-off and landing (VTOL) has become a capable and economical power source, due to its high energy and power densities, discharge rate (C-rate), and zero emission of pollutants (Donateo et al. (2017)). By considering a new and fully charged battery, the flight endurance is between 10 to 30 minutes (Roberts et al. (2008); Morbidi et al. (2016); Chang et al. (2016)), where 85% of the energy is consumed by the propulsion system. The remaining consumption is caused by the sensors, (such as GPS, accelerometers, compass, gyroscope (Aleksandrov and Penkov (2012))), the flight control computer, and for some payload (gimbal system, cameras, and other kind of sensors).

However, the flight endurance is gradually reduced over timer due to aging of the battery. The effect of aging is characterized by a capacity loss and immediately power fade. The aging is caused by several factors such as high-rate cycling, overdischarge and overcharge, and drastically changes of operation temperature (Watrin et al. (2012)). To avoid damages and reduce the aging rate during the charge/discharge cycles of the battery, it is necessary to monitor the State of Charge (SoC) and to establish safety limits around the End of Discharge (EoD) (also called *cut-off voltage*). At a given time, the SoC is the proportion of the available charge, compared to the total charge available when the battery is fully charged, it is analog to a car gas fuel gauge. On the other hand, the EoD indicates that the battery is fully discharged. In the literature of Electrical Cars, such concepts are the main criterion in the design of Battery Manage Systems (BMS) (Saha et al. (2011)), where the main objective is to define adequate operation regimes to extend the life of the battery and maximize the energy supplied. In the case of UAVs, the monitoring of SoC battery during the development of a mission will allow to establish a voltage safety limit before reaching the EoD to ensure the fulfillment of the mission, safeguard the integrity of the battery, and have an adequate use of the energy supplied to maximize the flight endurance.

Several researches have addressed the problem of flight endurance for different types of UAV considering mainly three types of powertrains such as batteries, fuel cells, and solar cells (Meyer et al. (2007); Saha et al. (2011); Swider-Lyons et al. (2011); Traub (2011)). The main objectives of such researches were the development of methodologies and strategies to increase the flight endurance taking into

⋆ This work was supported by CONACYT (Consejo Nacional de Ciencia y Tecnología)

account the geometry of the UAV, disturbance as the wind, the type of trajectory, the maximum altitude and the power requirement to perform a mission. In the specific case of multirotor UAVs powered by Li-Po batteries, the efforts have been focused to generate strategies to ensure the fulfillment of a mission and increase flight time, e.g. (De Souza Cândido et al. (2014)) are presented an integrated planning and control approach to increase the probability of completion of fly-by missions by battery-powered UAV quadrotor. The authors in (Abdilla et al. (2015a)) proposed a technique to extend the endurance of battery-powered rotorcraft by sub-diving the monolithic battery into multiple smaller capacity batteries which are sequentially discharged and released. Also, in (Abdilla et al. (2015b)) the authors characterized the power consumption of multirotors and derived an endurance estimation model. (Morbidi et al. (2016)) presented two optimal control problems with respect to the angular accelerations of four electrical motors of an UAV quadrotor to improve its flight endurance. More recently (Dietrich et al. (2017)) are presented experimental results of an analysis of the energy consumption and derivation and validation of empirical formulas to estimate the power consumption and the remaining flight time. The works mentioned above were mainly engaged in developing strategies to improve the consumption of the energy supply, which allows the battery to extend the power consumption for UAV applications, to extend the flight endurance and to ensure the fulfillment of a mission.

The main contribution of this work is to present a methodology to predict the flight endurance in the context of Prognosis & Health Management through a Model-based Prognosis algorithm based on the mathematical model of the propulsion system of an UAV multirotor. The prediction of flight endurance is developed in three sequential steps: 1) the estimation of the battery SoC through an Extended Kalman Filter, followed by 2) the propagation of the estimated SoC in the future until reaching a safety threshold value before the EoD, and the 3) update of the prediction. The proposed methodology is applied to an UAV hexarotor to demonstrate: i) the fulfillment of the UAV mission, ii) avoiding overdischarges in the battery, and iii) to be able to take decisions over the mission during the flight endurance prediction. Such considerations must be taken into account to perform routines of mission planning or trajectory reconfiguration. The remaining of the paper is organized as follows: The mathematical model of the propulsion system of an UAV multirotor is presented in the next section. The main concepts around Prognosis & Health Management and the Model-based Prognosis algorithm to predict the flight endurance are explained in Section 3. The development of the flight endurance is detailed in Section 4. The simulation results and the discussion are described in Section 5. Finally, the conclusion and perspectives of the future work are defined in the last Section.

2. MATHEMATICAL MODEL OF PROPULSION SYSTEM OF UAV MULTIROTOR

The propulsion system of a UAV multirotor is composed by a set of BrushLess DC Motors (BLDCM) powered by a Lithium Polymer battery as it can be seen in Fig. 1, where i denotes the *i-th* ESC-BLDCM. The connection

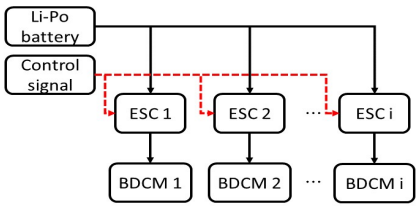

Fig. 1. Propulsion system of UAV multirotor.

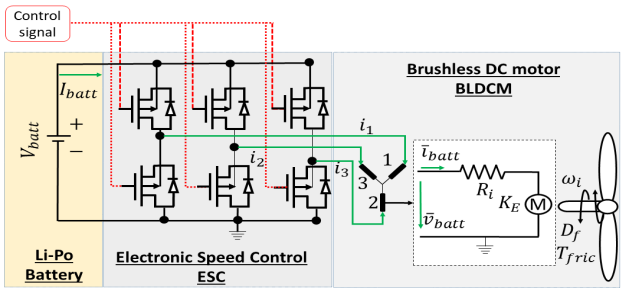

Fig. 2. Connexion of Li-Po battery - ESC - BLDCM.

between each motor and the battery is realized through an Electronic Speed Control (ESC). In Fig. 2 the connection between the Li-Po battery - ESC - BLDCM is detailed for one motor. The ESC adjusts the angular velocity of the BLDCM through a control signal which is a PWM signal. In this study the dynamic around the ESC is neglected and it is assumed that the voltage supply by the battery and the generated current by the motors are averaged with respect to the duty cycle value produced by the control signal.

2.1 Lithium Polymer battery model

Lithium Polymer (Li-Po) Batteries are devices converting the energy released by spontaneous chemical reaction to electricity work. Due to its rechargeable capability they belong to the Secondary Lithium batteries family and possess properties such as high discharge rate (C-rate), high energy and power densities (Julien et al. (2016)). A Li-Po battery is made up of several individual cells connected to each other in series (to have a high voltage value) or parallel (to have a high capacity in Ah). The battery model describes the mathematical relationship and evolution of voltage and State of Charge (SoC), which is in a given time the proportion of the charge available compared to the total charge available when it is fully charged. The range of the SoC is $SoC \in [\,0\ 1\,]$, where 1 corresponds to 100 % of the charge, i.e the battery is fully charged, and 0 indicates that the battery is fully discharge, i.e. the End of Discharge (EoD) or cut-off voltage value has been reached. The most used method to compute the SoC is the so called *Ampere Hour Counting* or *Coulomb Counting* (Gholizadeh and Salmasi (2014)):

$$SoC\,(t) = SoC\,(t_o) - \frac{1}{3600 \cdot C_T} \int_{t_o}^{t} I_{batt}(t)dt, \qquad (1)$$

where t_o represents the initial time, C_T is the total capacity of the battery expressed in (Ah). The mathematical model, describing the dynamic behavior of the voltage in a Li-Po battery or a single cell, is based on an Equivalent Circuit Representation (ECR) according to Fig. 3. The

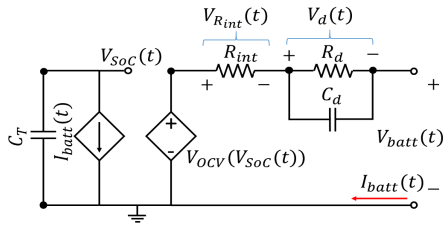

Fig. 3. Electrical equivalent circuit of a Lithium battery.

ECR was presented in (Chen and Rincon-Mora (2006)). In Fig. 3, (on the left-side of the circuit), the voltage $V_{SoC}(t)$ models the state of charge $SoC(t)$ of the battery from the capacity C_T. The voltage $V_{OCV}(V_{SoC})$ is the Open Circuit Voltage (OCV), i.e. it is the effective voltage in the terminals of battery, and it is modeled as a function of the state of charge of the battery. The voltage $V_{R_{int}}(t)$ characterizes the ohmic over-potential due to the internal resistance of the battery R_{int}. $V_d(t)$ represents the transitory response of the voltage when a current is demanding to the battery. It is characterized by a first order response and its time constant depends on the value of parameters R_d and C_d. The mathematical model of the battery is given by:

$$\begin{aligned} \dot{V}_{SoC}(t) &= -\frac{I_{batt}(t)}{3600 \cdot C_T} \\ \dot{V}_d(t) &= -\frac{V_d(t)}{R_d \cdot C_d} + \frac{I_{batt}(t)}{C_d} \\ V_{Batt}(t) &= V_{OCV}(V_{SoC}(t)) - V_d(t) - R_{int}\, I_{batt}(t), \end{aligned} \tag{2}$$

where, the $V_{OCV}(V_{SoC}(t))$ is defined experimentally as:

$$V_{OCV}(V_{SoC}(t)) = \sum_{i=0}^{n} \lambda_i V_{SoC}(t)^i + \ln(V_{SoC}) V_{SoC}(t) \tag{3}$$

It can be noted that, the nonlinear function (3) is not unique and its definition depends on the evolution of the battery dynamics and the magnitude of the discharge current. It is usually formulate using a polynomial function (Schacht-Rodriguez et al. (2017)), however in this work a logarithm term was added to model the final evolution of the battery voltage. To illustrate the voltage drop described previously, lets consider Fig. 4, where the demanded current and voltage of a new and fully charged Li-Po battery made up of four series-connected cells are shown. The battery was discharged before to reach the EoD value (established at 12 V) at room temperature. In Fig. 5 when the first current pulse is applied an immediately voltage drop caused by $V_{R_{int}}(t)$ occurs due to the internal resistance R_{int}. When the pulse is off, the voltage recovers by itself with a dynamic associated to $V_d(t)$ until reaching the open circuit voltage $V_{OCV}(V_{SoC})$.

As mentioned previously, the End of Discharge (EoD)

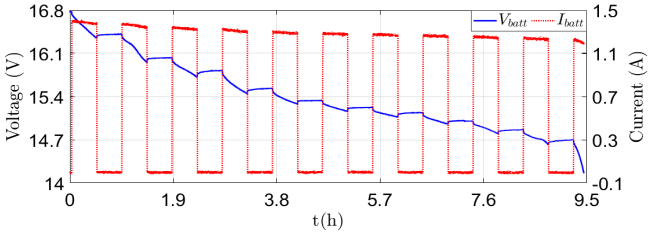

Fig. 4. Demanded Current and battery voltage at 25°C.

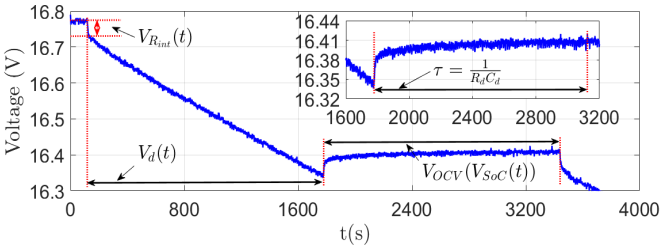

Fig. 5. Characteristics of the battery voltage.

is the cut-off voltage and it indicates that the battery is fully discharged. If this value is reached and the discharge continues, an irreversible damage is generated to the battery. One way to quantify the aging is to consider the State of Health (SoH). The SoH represents the actual conditions of a battery, in comparison with its nominal conditions. The main phenomena that characterizes the battery SoH is the capacity loss or capacity fade, which is caused by the reduction of the capacity value C_T according to the number of charge/discharge cycles (Cordoba-Arenas et al. (2013)). In Fig. 6, the aging effect in the voltage of a battery cell is shown. The battery cell was submitted to 150 charge/discharge cycles (N_{cycle}) (Saha and Goebel (2007)). The EoD was established at 2.6 V, and as it can be observed, the time to reach the EoD is reduced according to the number of charge/discharge cycles denoted by (N_{cycle}). The evolution of the numerical value of C_T, is plotted in Fig. 7. It can be noted that this evolution depends on the number of charge/discharge cycles (N_{cycle}), and the SoH can be defined as

$$\begin{aligned} SoH(N_{cycle}) &= \frac{C_a(N_{cycle})}{C_{int}} \\ C_T &= C_0 \cdot SoH(N_{cycle}), \end{aligned} \tag{4}$$

where $SoH(N_{cycle})$ is the SoH as an effect of capacity loss, $C_a(N_{cycle})$ is the value of the capacity in a specific charge/discharge cycle, and C_0 is the value of the capacity when the battery is new. Similar to SoC, the SoH is in a range of $SoH \in [\,0\ 1\,]$, i.e the SoH is 1 when the battery is new, and according to the use, damage, and other factors the SoH will be reduced.

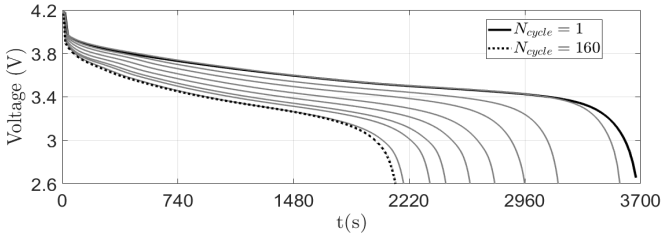

Fig. 6. Variation of voltage of a battery cell subject to 160 charge/discharge cycles (Saha and Goebel (2007)).

It can be noted that the decrease of the capacity affects directly the SoC and consequently the battery voltage (as it can be seen in equation (3)). This relationship is plotted in Fig. 8, where the dependence between the SoC and the battery voltage is shown. In that sense, the time when the EoD is reached can be determinate when the SoC reaches 0. It should be mentioned that one characteristic in the dynamic associated to the battery voltage during a discharge is the exponential fall of the voltage before

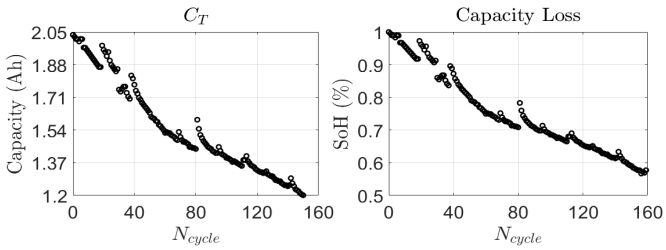

Fig. 7. Capacity loss and battery SoH (Saha and Goebel (2007)).

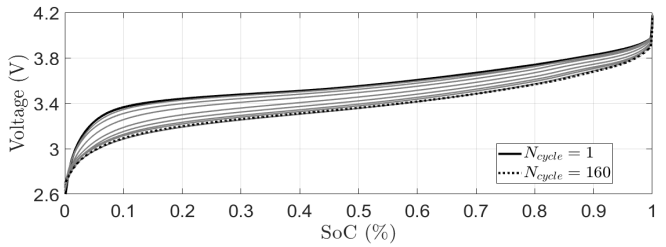

Fig. 8. Relationship between battery voltage and SoC.

reaching the EoD. The voltage fall can be seen in Fig. 8, which occurs after the SoC reach the 0.1 %.

2.2 BrushLess DC Motor

The mathematical model of the BrushLess DC Motor (BLDCM) is divided into the electrical and the mechanical sub-models described by the following equations (Moseler and Isermann (2000)):

$$\bar{v}_{batt}(t) = R\bar{i}_{batt}(t) + K_E\omega(t),$$
$$\dot{\omega}(t) = \frac{K_E}{J_{TP}}\bar{i}_{batt}(t) - \frac{d}{J_{TP}}\omega^2(t) + \frac{D_f}{J_{TP}}\omega(t) - \frac{T_{fric}}{J_{TP}}, \quad (5)$$

where $R = \frac{2}{3}(\sum_{i=1}^{3} R_i)$ is the equivalent electric resistance of each coil, K_E is the back electromotive force, $\omega(t)$ is the angular velocity, T_{fric} is the motor friction torque, D_f is the viscous damping coefficient of the motor, d is the drag constant, associated to the geometry of the propeller, and J_{TP} is the inertia of the motor. The average voltage $\bar{v}_{batt}(t)$ and current $\bar{i}_{batt}(t)$ are the voltage and current generated by the ESC and they are computed as follows:

$$\bar{v}_{batt}(t) = V_{batt}(t) \cdot D_{cycle}$$
$$I_{batt}(t) = \bar{i}_{batt}(t) \cdot D_{cycle}, \quad (6)$$

where $V_{batt}(t)$ is the battery voltage, $I_{batt}(t)$ is the current generated by the motors, and D_{cycle} is the duty cycle of Pulse-Width Modulation (PWM) signal, which corresponds to control signal of the motor speed. D_{cycle} can be defined as a function of the square of the angular velocity of the motors and it is determined through experimental correlations, such as $D_{cycle} = f(\omega(t)^2)$.

3. PROGNOSIS & HEALTH MANAGEMENT

According to (Goebel et al. (2017); Kim et al. (2017)) the Prognosis & Health Management (PHM) is a novel engineering approach which enables the health assessment of a system according to its actual operating conditions, as well as the prediction of its future condition based on up to date information. One of the main objectives of the PHM is to predict how the system will behave in the future in order to know if more stress or changes in the nominal operation on the system will likely cause an acceleration towards a certain undesirable *event* or *failure condition*, and the time when such event will occurs. In order to illustrate how

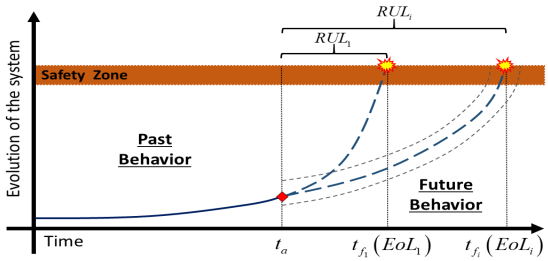

Fig. 9. Evolution of the system behavior.

the prognosis is performed, let us consider Fig. 9. The solid dark blue line represents the past evolution of the system behavior until present time t_a, and the brown area is the *Safety Zone (SZ)* or the nominal operational limit. According to different factors such as the inputs of the system, aging, or even external disturbances, the system behavior could be progress until reach values outside of its nominal operation. In that sense, if such factors are known, the future trajectory of the system behavior can be predicted until reaching the SZ (segmented blue lines). In the prognosis literature, the *End of Life (EoL)* is reached, when the system behavior reaches or exceed the upper limit of the SZ at some time t_{f_i}, and the *Remaining Useful Time (RUL)* until reach the EoL is computed as

$$RUL_i = t_{f_i}(EoL_i) - t_a. \quad (7)$$

In this work, the system under study is the propulsion system of an UAV multirotor. In that sense, several characteristics of the system behavior could be predicted, such as: i) the battery SoC in a given time. ii) the fulfillment of a mission before to reach the EoD, iii) the flight endurance of the UAV and the Remaining Mission Time. In this work the RUL is considered as the RMT of the UAV.

3.1 Model-based Prognosis

Depending on the accuracy level of the prediction and the complexity of the system behavior, different approaches have been used to perform prognosis (Goebel et al. (2017); Coble (2010)). The Model-based Prognosis or Condition-based Prediction assess the behavior of individual components of a system as well as the entire system based on a mathematical model that describe the evolution of some system variables (i.e temperature, voltage, position, speed) over time. If such mathematical model exists, the future behavior of the system can be determinate by propagating the mathematical model in the future time. However, to determinate a mathematical model of the interested system in order to perform a prediction of its future behavior is not a trivial task. First, it is necessary to define which system variables are necessary to evaluate the entire system behavior, and determine if such variables are directly measured or not. If such variables are measured, a mathematical model can be defined and used to perform the prediction in the future time. Otherwise, if such variables are unmeasured, they must be estimated. In that sense, this work presents in Fig. 10 a Model-based Prognosis methodology based on an estimation of the battery SoC in order to predict the flight endurance of

the UAV. The prediction is developed in three sequential steps: 1) estimation of unmeasured states of the system, 2) propagation and prediction of the estimated state, and 3) update of the prediction.

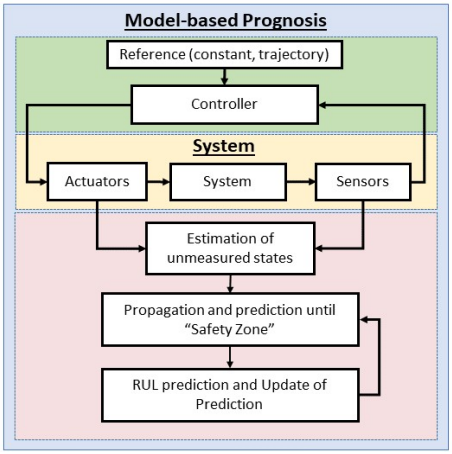

Fig. 10. Model-based Prognosis methodology.

State Estimation. In several dynamic systems, not all state variables can be measured. For such cases, an observer needs to be designed in order to estimate the unmeasured states considering the system model and the available input-output signals. In this work an Extended Kalman Filter (EKF) is used to estimate the battery SoC. The EKF has demonstrated to be an adequately tool to estimate the battery states as well as parameters in battery systems (Plett (2004); He et al. (2011)). In this work the EKF is developed considering a simplified mathematical model where the unique nonlinear term is the Open Circuit Voltage. The EKF addressed the general problem of state estimation of a nonlinear system, expressed in discrete time as:

$$\begin{aligned} x_{k+1} &= f(x_k, u_k) + w_k \\ y_k &= g(x_k, u_k) + v_k, \end{aligned} \tag{8}$$

where $f(x_k, u_k)$ and $g(x_k, u_k)$ are the nonlinear state transition function and nonlinear measurement function, respectively, and they are assumed to be differentiable at each operating point. The random variables $w(t)$ and $v(t)$ are the process and measurement noise. They are assumed to be independent, white, and with normal probability distributions:

$$\begin{aligned} p(w) &\sim \quad N(0, Q) \\ p(v) &\sim \quad N(0, R). \end{aligned} \tag{9}$$

The matrices Q and R are the process noise covariance and measurement noise covariance, respectively. At each sample time, $f(x_k, u_k)$ and $g(x_k, u_k)$ are linearized through a first-order Taylor-series developed as

$$A = \left.\frac{\partial f(x_k, u_k)}{\partial x_{k-1}}\right|_{x_{k-1}=\hat{x}_{k-1}^-} \tag{10}$$

$$C = \left.\frac{\partial g(x_k, u_k)}{\partial x_k}\right|_{x_k=\hat{x}_k^-} \tag{11}$$

The completed equations of the EKF are resumed in Algorithm (1).

Algorithm 1 Extended Kalman Filter algorithm Plett (2004).

Initial values of $\hat{x}_{k-1}^-$ and P_{k-1}
To compute:

$$A_k = \left.\frac{\partial f(x_k, u_k)}{\partial x_{k-1}}\right|_{x_{k-1}=\hat{x}_{k-1}^-}$$

$$C_k = \left.\frac{\partial g(x_k, u_k)}{\partial x_k}\right|_{x_k=\hat{x}_k^-}$$

State estimate update:

$$\hat{x}_k^- = f(\hat{x}_{k-1}, u_{k-1}),$$

Error covariance matrix:

$$P_k^- = A_k P_k A_k^{\mathsf{T}} + Q,$$

Kalman gain:

$$K_k = P_k^- C_k^{\mathsf{T}} (C_k P_k^- C_k^{\mathsf{T}} + R)^{-1},$$

State estimate measurement update:

$$\hat{x}_k = \hat{x}_k^- + K_k(y_k - g(\hat{x}_k^-, u_k)),$$

Error covariance matrix update:

$$P_k = (I - K_k C_k) P_k^-.$$

Propagation and Prediction of estimated states. As mentioned previously, if a mathematical model that describes the evolution of system behavior as a function of the time exists, the prediction of future behavior can be determined by propagating the model in the future time. However if the system involves unmeasured variables, they must be estimated first, and the prediction of its future behavior is based on the propagation of the estimated variables in the future. In order to illustrate how the propagation and prediction are performed, let us consider Fig. 9 where the trend of the past evolution of system behavior at time t_a is known. It is possible to define a function that approximate the trend with the time, and propagate the function in the future until reaches the SZ. This function is called *prediction function*, and the accuracy of the prediction will depend on the amount of past data measure. On the other hand, the prediction function can be updated by using new data of the system. Due to the fact that there are no abrupt changes or discontinuities in the evolution of estimation SoC, the prediction function is defined as a polynomial function of the time, such as:

$$\eta\,(t, \alpha) = \sum_{j=0}^{m} \alpha_j . t^j = \alpha_0 + \alpha_1 \cdot t + \cdots + \alpha_m \cdot t^m, \tag{12}$$

where $\eta(t)$ represents the predicted variable, t is the time, α_i are identified parameters associated to measured data trend and m is the order of the polynomial function. The method of *Weighted Least Squares (WLS)* is considered to estimate the parameters (α_i) of (12). The WLS is defined as:

$$\begin{aligned} \mathrm{H} &= [\,1 \;\; t \;\cdots\; t^m\,], \\ \hat{\alpha} &= [\mathrm{H}^{\mathrm{T}}\mathrm{R}^{-1}\mathrm{H}]^{-1}\mathrm{H}^{\mathrm{T}}\mathrm{R}^{-1}\mathrm{Y}, \end{aligned} \tag{13}$$

where H contains the information of the relationship between the time and the polynomial order, $\hat{\alpha}$ is the vector with the estimated parameters α_i, R is the measurement covariance matrix, and Y is the vector of the measured data (variable to be identified). The approximation is

evaluated according to the coefficient of determination R^2, which is limited as $R^2 \in [\,0.9\ 1\,]$ in this study, and the polynomial order depends on the accuracy between the data and the identified function. The iterative sequence of propagation and prediction is given in the Algorithm 2.

Algorithm 2 Propagation and prediction algorithm.

(1) Delay (t_p)

(2) Recollect data until $\hat{SoC}(t_a)$

(3) Define H and m for

$$\mathrm{H} = [\,1\ t\ \cdots\ t^m\,]$$

and

$$\eta\,(t,\alpha) = \sum_{j=0}^{m} \alpha_j.t^j = \alpha_0 + \alpha_1 \cdot t + \cdots + \alpha_m \cdot t^m$$

(4) Estimate $\hat{\alpha}$ with $Y = \hat{SoC}(t_0 : t_a)$

$$\hat{\alpha} = [\mathrm{H^T R^{-1} H}]^{-1}\mathrm{H^T R^{-1} Y}$$

(5) Verify $\mathbf{R}^2$ to $Y = \hat{SoC}(t_0 : t_a)$ with $\eta\,(t_0 : t_a, \hat{\alpha})$

(6) Propagate $\eta\,(t_0 : t_a, \hat{\alpha})$ until $t(SVT)$ to determinate the Flight Endurance (FE)

$$FE = t(SVT)$$

(7) Compute *Remaining mission Time (RMT)*

$$RMT = t(SVT) - t_a$$

4. PREDICTION OF FLIGHT ENDURANCE OF UAV MULTIROTOR

The methodology explained previously will be applied to predict the flight endurance of an UAV hexarotor. During the development of a mission of some UAV, the End of Discharge (EoD) must be taking into account to ensure the safety of the UAV, the fulfillment of the mission, and the maximization of flight endurance. In that sense, the total flight endurance is considered as the time between the beginning of the mission until reaches a *Safety Voltage Threshold* before EoD value. Several factors are implied in the flight endurance of the UAV, such as the total current demanded by the number of the BLDCM ($I_{batt}(t)$), and C-Rate, the rate discharge (C), the initial charge $SoC(t_0)$, and the State of Health SoH. Then, assuming a new and fully charged battery, the EoD is directly associated with the battery voltage. The time when EoD is reached can be computed considering the demanded current ($I_{batt}(t)$) through relation of C-Rate discharge. However according to the number of charge/discharge, the capacity of the battery decreases and the discharge rate is modified as the aging of the battery increases. In that sense, the computing of EoD time should consider the effect of the aging to obtain the total flight endurance according to the battery SoH. As it can be observed from (2), the variation of C_T affects directly the SoC and consequently the OCV(3). Then, considering the relationship between the battery voltage and the SoC shown in Fig. 8, the EoD can be directly associated to the SoC. Taking into account that the total current demanded by the set of BLDCM is known or measure, the SoC of the battery during the mission can be computed using equation (1) or estimated through EKF, and its future trajectory can be propagated and predicted in the future until reaching the EoD, leading to prediction of the flight endurance. The development of each step in the PHM architecture shown in Fig. 10 to predict the flight endurance of the UAV is explained in the next section.

4.1 SoC estimation

The prediction of the flight endurance is based on the computation or estimation the battery SoC during the UAV mission. In that sense, two cases are considered in this work: 1) the direct computation of the SoC using the Amper counting method, and 2) the estimation of the SoC using a EKF. In the first case, the SoC is computed directly using equation (1). However, this method accumulates errors in measurements and may lead to large SoC errors in real-world applications (Gholizadeh and Salmasi (2014)). In that sense, the estimation of SoC is considered based on the design of an Extended Kalman Filter applied on system (2).

EKF of Li-Po battery. The estimation of SoC is developed according to Algorithm 1. System (2) is discretized through forward Euler method, and rewriting in state space:

$$\begin{aligned} x_{k+1} &= \begin{bmatrix} 1 & 0 \\ 0 & 1 - \dfrac{T_s}{R_d C_d} \end{bmatrix} x_k + \begin{bmatrix} -\dfrac{T_s}{C_T} \\ \dfrac{T_s}{C_d} \end{bmatrix} u_k + w_k \\ y_k &= \begin{bmatrix} \dfrac{\partial V_{OCV}\,(V_{SoC})}{\partial V_{SoC}^-} & -1 \end{bmatrix} x_k - R_{int} u_k + v_k, \end{aligned} \tag{14}$$

where the discrete state space vector is $x_k = [\,V_{SoC}\ V_d\,]^{\mathrm{T}}$, the input $u_k = I_{batt}$, the output $y_k = V_{batt}$, and T_s is the sampling time. The nonlinear term is the OCV shown in equation (1), which is in the matrix C. The variation in the measurement and process noise are established at $\pm 0.1\,V$, and $\pm 0.01\,V$ and the process and measurement covariance matrices are defined using experimental data from a real battery (Schacht-Rodriguez et al. (2017)) as:

$$\begin{aligned} Q &= \begin{bmatrix} 1 \times 10^{-2} & 0 \\ 0 & 1 \times 10^{-2} \end{bmatrix} \\ R &= [\,0.1\,]\,. \end{aligned} \tag{15}$$

The propagation and prediction of the estimated SoC is developed according to Algorithm (2). It is important to mention that the methodology shown in Fig. 10, considers two types of sampling time during its implementation, i.e. whiles the state estimation stage is subject to the sampling time of the system in order of milliseconds, the propagation and evaluation could be performed in a sampling time in the order of seconds, or even minutes.

5. RESULTS AND DISCUSSION

The methodology introduced in this paper to predict the flight endurance was tested in simulation considering the propulsion system of an UAV hexarotor. A Li-Po battery of four cells was considered as powertrain and the parameters were obtained using experimental data considering the methodology presented in (Schacht-Rodriguez et al. (2017)). Considering the relationship between the battery voltage and the SoC, the SVT is defined according to Fig. 11. As it can be observed, before the voltage reaches the EoD, there is an abrupt exponential fall of voltage.

Taking into account this phenomena, the SVT is defined before the voltage reaches the EoD. The UAV was sub-

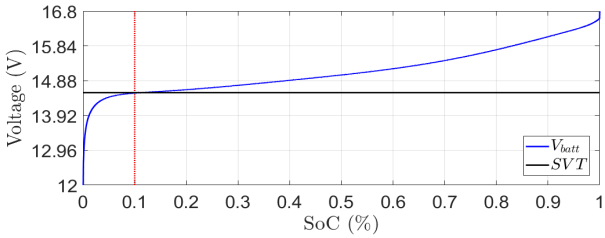

Fig. 11. Safety Voltage Threshold of the Li-Po battery.

jected to a mission which consisted in following circular trajectory with an area of 785400 m^2 around $x-y$ axis and an altitude of 20 m (Fig. 12). Such trajectory was developed considering the mathematical model of UAV presented in (Arellano-Muro et al. (2013)). Considering that the battery is fully charged and new, the initial SoC and SoH were established in 1 respectively. The current

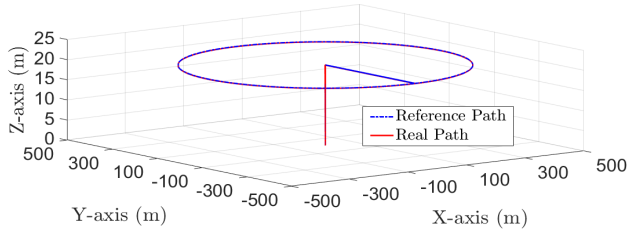

Fig. 12. 3D Path of UAV hexarotor.

generated by the six motors is shown in Fig. 13-(a). The variations in the current are due to velocity changes of the motors caused by the UAV movement. The comparison between the voltage battery and its estimation is observed in Fig. 13-(b). As it can be seen, the mission is fulfilled in 20 minutes before to reach the SVT,and this avoided an overdischarge in the battery. The comparison between the estimated SoC through the EKF and the computed SoC by Coulomb Counted is shown in Fig. 14. As it can be noted, the SoC estimation through the EKF relates the SoC with the dynamic of the battery discharge. This relationship allows to predict the flight endurance from the estimated SoC.

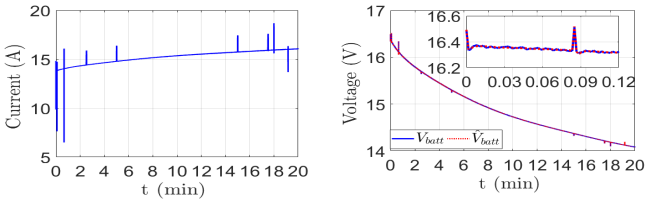

(a) (b)

Fig. 13. (a) Demanded current I_{batt} and (b) comparison of V_{batt} and $\hat{V}_{batt}$.

The propagation and prediction was developed over sampling time of 1 minute, and the SoC estimation each 10 milliseconds to collect enough data to estimate the parameters of the prediction function (12). Two 1^{st} and 2^{nd} order polynomials were considered for the prediction function.

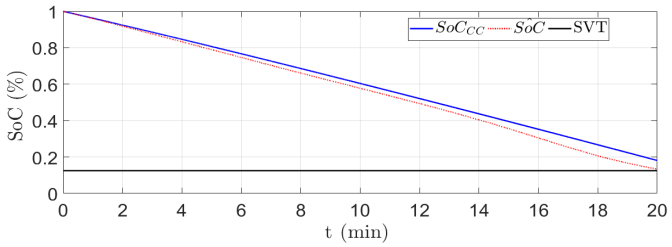

Fig. 14. Comparison between SoC_{CC} and $\hat{SoC}$.

The predictions of the total flight endurance for both prediction functions are plotted in Fig. 15. The blue marks correspond to the predicted flight endurance with the 1^{st} order polynomial, and the red marks with the 2^{nd} order polynomial. As it can be observed, the first predictions ($1-4$ min) with the 1^{st} order polynomial are closer to the real flight endurance, whilst an approximation of the real flight endurance is displayed from 6 minute onwards with the 2^{nd} order polynomial. However the closest prediction of real flight endurance is obtained at time 8 min with the 2^{nd} order polynomial. In Fig. 16 and Fig. 17 the results of

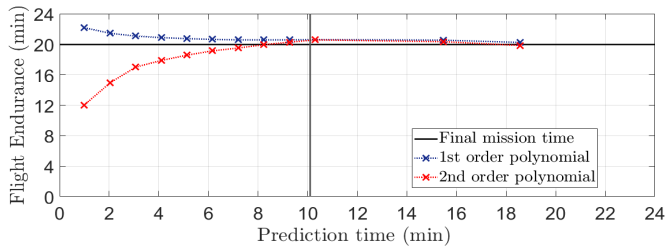

Fig. 15. Flight Endurance prediction.

the prediction for the 1^{st} and 2^{nd} order polynomial at time 1, 6 and 8 min, and their comparison with the estimated SoC are shown. A *Decision Threshold (DT)* at the 0.6% (at time 10 min of the total flight endurance) of estimated SoC was defined to determinate an operation range where the predictions will be useful to take decisions on the progress of the mission. The computation of Remaining Mission Time (RMS) was made from the first prediction, and the results are shown in Fig. 18. As it can be seen, it is possible to predict the total flight endurance and the RMS from the beginning of the mission considering the defined DT.

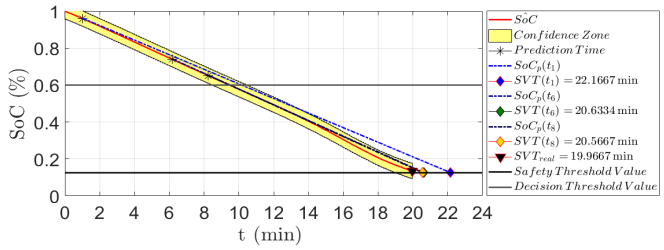

Fig. 16. Prediction of FE with 1^{st} order polynomial.

6. CONCLUSION AND FUTURE WORKS

In this paper, a methodology based on a Model-based Prognosis was employed to predict the flight endurance and remaining mission time of a class of multirotor UAVs. Through an Extended Kalman Filter the battery SoC was estimated, and using a polynomial function, the estimated

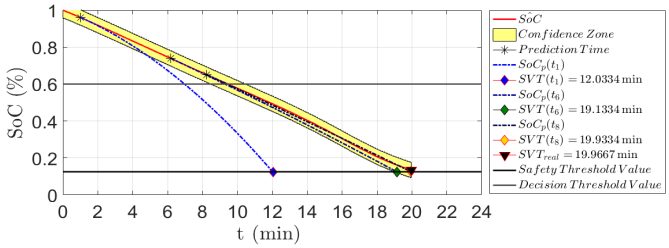

Fig. 17. Prediction of FE with 2^{st} order polynomial.

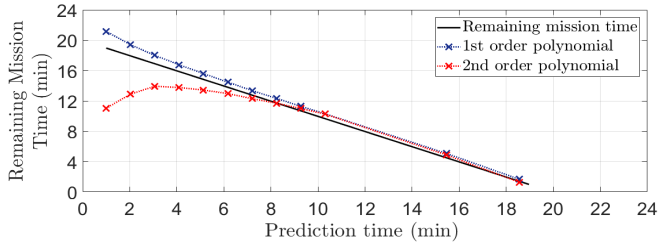

Fig. 18. Evolution of Remaining Mission Time.

SoC was propagate in the future time before reaching the EoD. The propagation and prediction algorithm presented can be applied on other type of electrically powered UAV. On the other hand, the prognosis methodology also enabled to define safe operating limits in the battery to avoid damages and guarantee the fulfillment of the UAV mission. The simulation results exhibited that it is possible to predict the total flight endurance and the remaining mission time before the end of the mission considering a Decision Threshold between the beginning of the mission and the time when the prediction is closest with the real value. The Decision Threshold is necessary in order to define a scheme of Decision Making for mission planning or trajectory planning. In that sense, the prediction of the flight endurance will be the core of a path planning and re-planning strategy to take actions over the evolution of a mission as future work.

REFERENCES

Abdilla, A., Richards, A., and Burrow, S. (2015a). Endurance Optimisation of Battery-Powered Rotorcraft. In *Conference Towards Autonomous Robotic Systems*, 1–12. Springer.

Abdilla, A., Richards, A., and Burrow, S. (2015b). Power and endurance modelling of battery-powered rotorcraft. In *Intelligent Robots and Systems (IROS), 2015 IEEE/RSJ International Conference on*, 675–680. IEEE.

Aleksandrov, D. and Penkov, I. (2012). Energy consumption of mini UAV helicopters with different number of rotors. In *11th International Symposium" Topical Problems in the Field of Electrical and Power Engineering*, 259–262.

Arellano-Muro, C.A., Luque-Vega, L.F., Castillo-Toledo, B., and Loukianov, A.G. (2013). Backstepping control with sliding mode estimation for a hexacopter. In *Electrical Engineering, Computing Science and Automatic Control (CCE), 2013 10th International Conference on*, 31–36. IEEE.

Chang, K., Rammos, P., Wilkerson, S., Bundy, M., and Gadsden, S.A. (2016). LiPo battery energy studies for improved flight performance of unmanned aerial systems. In *SPIE Defense+ Security*, 98370W–98370W. International Society for Optics and Photonics.

Chen, M. and Rincon-Mora, G.A. (2006). Accurate electrical battery model capable of predicting runtime and IV performance. *IEEE transactions on energy conversion*, 21(2), 504–511.

Coble, J.B. (2010). Mergin data sources to predict remaining useful life - an automated method to identify prognostic parameters.

Cordoba-Arenas, A., Onori, S., Rizzoni, G., and Fan, G. (2013). Aging Propagation in Advanced Battery Systems: Preliminary Results. *IFAC Proceedings Volumes*, 46(21), 313–318.

De Souza Cândido, A., Galvão, R.K.H., and Yoneyama, T. (2014). Control and energy management for quadrotor. In *Control (CONTROL), 2014 UKACC International Conference on*, 343–348. IEEE.

Dietrich, T., Krug, S., and Zimmermann, A. (2017). An empirical study on generic multicopter energy consumption profiles. In *Systems Conference (SysCon), 2017 Annual IEEE International*, 1–6. IEEE.

Donateo, T., Ficarella, A., Spedicato, L., Arista, A., and Ferraro, M. (2017). A new approach to calculating endurance in electric flight and comparing fuel cells and batteries. *Applied Energy*, 187, 807–819.

Gholizadeh, M. and Salmasi, F.R. (2014). Estimation of state of charge, unknown nonlinearities, and state of health of a lithium-ion battery based on a comprehensive unobservable model. *IEEE Transactions on Industrial Electronics*, 61(3), 1335–1344.

Goebel, K., Dagle, M., Saxena, A., Sankararama, S., Roychoudhury, I., and Celaya, J.R. (2017). *PROGNOSTICS The Science of Prediction*.

He, H., Xiong, R., Zhang, X., Sun, F., and Fan, J. (2011). State-of-Charge estimation of the lithium-ion battery using an adaptive extended Kalman filter based on an improved Thevenin model. *IEEE Transactions on Vehicular Technology*, 60(4), 1461–1469.

Julien, C., Mauger, A., Vijh, A., and Zaghib, K. (2016). Lithium batteries. In *Lithium Batteries*, 29–68. Springer.

Kim, N.H., An, D., and Choi, J.H. (2017). *Prognostics and Health Management of Engineering Systems*. Springer.

Meyer, J., Du Plessis, J., Ellis, P., and Clark, W. (2007). Design considerations for a low altitude long endurance solar powered unmanned aerial vehicle. In *AFRICON 2007*, 1–7. IEEE.

Morbidi, F., Cano, R., and Lara, D. (2016). Minimum-Energy Path Generation for a Quadrotor UAV. In *IEEE International Conference on Robotics and Automation*.

Moseler, O. and Isermann, R. (2000). Application of model-based fault detection to a brushless DC motor. *IEEE Transactions on industrial electronics*, 47(5), 1015–1020.

Plett, G.L. (2004). Extended Kalman filtering for battery management systems of LiPB-based HEV battery packs: Part 3. State and parameter estimation. *Journal of Power sources*, 134(2), 277–292.

Roberts, J.F., Zufferey, J.C., and Floreano, D. (2008). Energy management for indoor hovering robots. In *2008 IEEE/RSJ International Conference on Intelligent Robots and Systems*, 1242–1247. IEEE.

Saha, B. and Goebel, K. (2007). Battery data set. *NASA AMES prognostics data repository*.

Saha, B., Koshimoto, E., Quach, C.C., Hogge, E.F., Strom, T.H., Hill, B.L., Vazquez, S.L., and Goebel, K. (2011). Battery health management system for electric UAVs. In *Aerospace Conference, 2011 IEEE*, 1–9. IEEE.

Schacht-Rodriguez, R., Ortiz-Torres, G., García-Beltrán, C., Astorga-Zaragoza, C., Ponsart, J., and Theilliol, D. (2017). SoC estimation using an Extended Kalman filter for UAV applications. In *Unmanned Aircraft Systems (ICUAS), 2017 International Conference on*, 179–187. IEEE.

Swider-Lyons, K.E., MacKrell, J.A., Rodgers, J.A., Page, G.S., Schuette, M., and Stroman, R.O. (2011). Hydrogen fuel cell propulsion for long endurance small uavs. In *The AIAA centennial of naval aviation forum*, volume 100.

Traub, L.W. (2011). Range and endurance estimates for battery-powered aircraft. *Journal of Aircraft*, 48(2), 703–707.

Watrin, N., Blunier, B., and Miraoui, A. (2012). Review of adaptive systems for lithium batteries State-of-Charge and State-of-Health estimation. In *2012 IEEE Transportation Electrification Conference and Expo (ITEC)*, 1–6. IEEE.